THE JOURNAL OF PHYSICAL CHEMISTRY C

Article

pubs.acs.org/JPCC

An Atomic-Scale View of the Nucleation and Growth of Graphene Islands on Pt Surfaces

Xiaofeng Feng,[†,‡] Jason Wu,[§] Alexis T. Bell,[§] and Miquel Salmeron*[,†,‡]

[†]Materials Sciences Division, Lawrence Berkeley National Laboratory, Berkeley, California 94720, United States

[‡]Department of Materials Science and Engineering and [§]Department of Chemical and Biomolecular Engineering, University of California, Berkeley, Berkeley, California 94720, United States

ABSTRACT: We study the nucleation and growth of epitaxial graphene on Pt(111) surfaces at the atomic level using scanning tunneling microscopy (STM). Graphene nucleation occurs both near Pt step edges and on Pt terraces, producing hexagonally shaped islands with atomically sharp zigzag edges. Graphene interacts strongly with Pt substrate during growth, by etching and replacement of Pt atoms from step edges, which results in faceting of the Pt steps. The favorable lattice orientations of graphene islands are found to be parallel to those of the Pt substrate, but other orientations are still possible. Grain boundaries are formed when two graphene islands merge with different lattice orientations. Improved growth conditions such as smaller nucleation density and higher growth rate can produce high-quality graphene film with larger grain sizes.

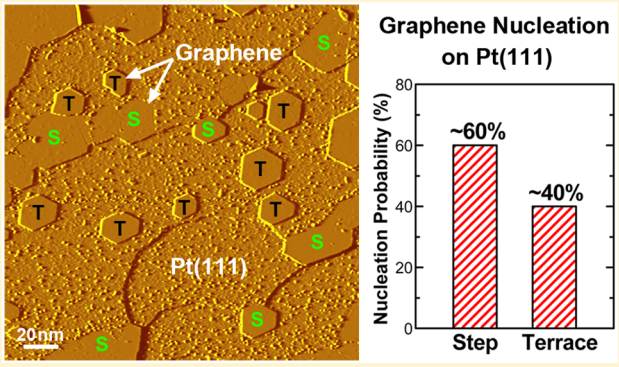

1. INTRODUCTION

Graphene, a single layer of graphite, has recently attracted extensive attention due to its extraordinary physical and chemical properties, making it a promising material for numerous applications.[1] Currently, the major bottleneck for graphene applications lies in the controlled synthesis of large-area, high-quality graphene films. Epitaxial graphene on metal substrates (e.g., Ru, Cu, Ni, and Pt) has been demonstrated to be a promising route.[2−6] Thus, numerous efforts have been made to understand the growth mechanism of graphene on metal substrates.[7−17] For example, the nucleation of graphene islands has been explored by Gao et al. using density functional theory (DFT) calculations,[8] indicating that nucleation near a metal step edge is more likely than on a terrace. Using low-energy electron microscopy (LEEM), Loginova et al. measured the growth rate of graphene islands on Ru(0001) and suggested that graphene grows by adding carbon clusters of about five atoms.[10] Growth intermediates prior to graphene formation, such as carbon dimers, carbon rectangles, and carbon chains, have been identified by using scanning tunneling microscopy (STM).[12] The strong interactions of graphene with metal substrate during graphene growth, such as metal etching effect, has also been revealed by LEEM and STM.[13]

From a catalysis point of view, the formation of graphene films on catalyst metal surface is undesired because the graphene layers coat the catalyst, which prevents the adsorption of reactant species and leads to catalyst deactivation.[18] For example, Pt nanoparticles are active catalysts for alkane dehydrogenation but exhibit a high tendency for coke formation.[19] Transmission electron microscopy (TEM) observation suggested that graphene formation initiates at low-coordination number sites located at steps on the surface of Pt nanoparticles.[20] Interestingly, the addition of Sn or In atoms to Pt can reduce coke formation, as they might inhibit the formation of carbon films on Pt surfaces.[19,21] In order to better understand how promoters help achieve a more stable catalyst, a more thorough understanding of carbon growth on the monometallic Pt catalyst is needed. At the same time, the decomposition and conversion of ethylene to carbon clusters and graphene films on Pt substrates have been studied by STM[22−26] to obtain a better understanding of carbon-producing surface reactions on metal surfaces, with the goal of controlling coke formation in heterogeneous catalysis.

The present study aims at extending the existing knowledge on graphene nucleation and growth on metal surfaces and providing details on the atomic-level interactions between graphene and metals using STM. The nucleation and growth of graphene on Pt(111) was prepared by the adsorption of a monolayer ethylene followed by annealing to 1223 K, producing hexagonal graphene nanoislands. A quantitative statistics of the graphene nucleation sites (step vs terrace) was acquired. The graphene growth resulted in faceting of the Pt steps, indicating a strong graphene−metal interaction during growth. The formation of grain boundaries in graphene films was also discussed. The results contribute to a deeper

Received: December 6, 2014
Revised: March 16, 2015
Published: March 17, 2015

DOI: 10.1021/jp512163n
J. Phys. Chem. C 2015, 119, 7124−7129

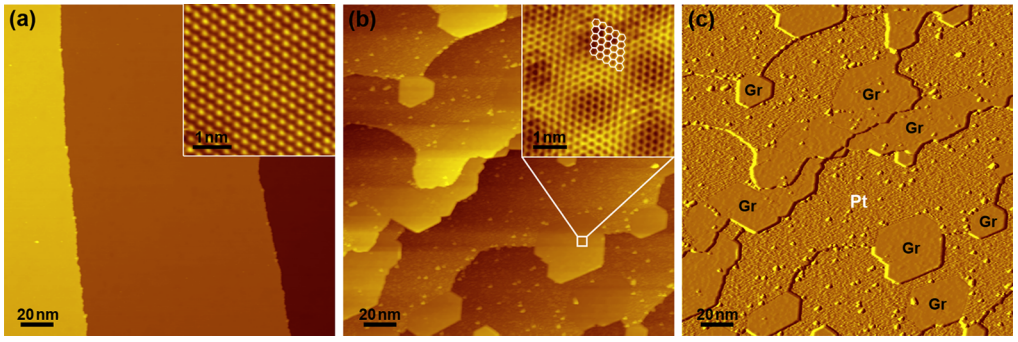

Figure 1. STM images showing graphene nucleation on flat Pt(111) substrate prepared using method 1. (a) STM image of the clean Pt(111) surface with atomic structure resolved in the inset. (b) STM topography and (c) derivative image of the Pt surface after graphene nucleation at 1223 K. Graphene islands (smooth areas) are found and can be distinguished easily in the derivative image (c). The atomic structure of a graphene island is shown in the inset of (b). Imaging parameters: (a) sample bias voltage V_s = 200 mV, tunneling current I_t = 15 pA; (inset) V_s = 27 mV, I_t = 200 pA; (b) V_s = 300 mV, I_t = 14 pA; (inset) V_s = 20 mV, I_t = 400 pA.

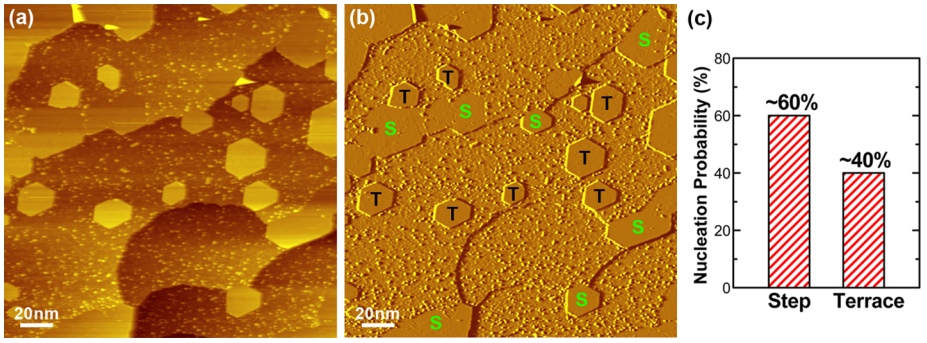

Figure 2. STM topography (a) and derivative (b) images showing the nucleation of graphene islands on the flat Pt(111) substrate using growth method 1. The hexagonal graphene islands are clearly visible in (b), which are marked with "S" or "T" according to their locations (near a step edge or on a terrace). Imaging parameters: V_s = 300 mV, I_t = 14 pA. (c) Statistical data over 300 graphene islands indicate that about 60% of them are located near a step and 40% are on top of a terrace.

understanding of graphene nucleation and controlled growth on metal surfaces.

2. EXPERIMENTAL SECTION

The experiments were performed using a home-built, low-temperature ultrahigh-vacuum (UHV) STM operated at a base pressure below 5×10^{-11} Torr.[27] Two Pt samples were used in this study: one is a flat Pt(111) single crystal from MaTeck with broad terraces (>100 nm), and the other is a stepped Pt(111) single crystal from Metal Crystals & Oxides Ltd. with narrow terraces (~3 nm). Both samples were cleaned through cycles of degassing at 1323 K, annealing in oxygen, and Ar ion sputtering at 1 keV. The long-term stability and cleanness of the samples were confirmed by both STM and Auger electron spectroscopy. After Ar ion sputtering, the samples were annealed to 1173 K under vacuum before graphene growth. Two methods were used to prepare graphene on Pt. Growth method 1: expose the Pt sample to ethylene (2×10^{-7} Torr) at room temperature to saturate the surface with hydrocarbons and subsequently anneal it to 1223 K under vacuum for 10 min to form graphene. This method was developed to capture the initial nucleation stage of graphene. Graphene growth at lower annealing temperatures (1073–1173 K) was also tried, which resulted in graphene islands with similar structures but lower crystallinity. Growth method 2: directly expose the Pt sample to ethylene (2×10^{-7} Torr) at 1223 K for 2 min to produce large-area graphene films. The sample was then transferred to the STM station in a connected UHV chamber. All STM images presented in this paper were acquired at 77 K.

3. RESULTS AND DISCUSSION

Figure 1a shows an STM image of the flat Pt(111) surface with atomically resolved lattice in the inset. The Pt surface exhibits broad terraces (>100 nm) with relatively smooth step edges. After the adsorption of ethylene at room temperature followed by annealing to 1223 K, distinct islands with hexagonal boundaries (forming 120°) were found near the steps (Figure 1b). Atomically resolved image is shown in the inset revealing the honeycomb lattice of graphene in the islands. The rest of the Pt surface was covered by clusters, likely due to carbonaceous species arising from hydrocarbon decomposition not yet incorporated into crystalline graphene islands.[12] These clusters are typically 1–3 nm in diameter, similar to the clusters formed after ethylene dehydrogenation shown in previous reports.[24,26] The contrast between graphene islands and Pt surfaces covered by carbon clusters is more apparent in the derivative STM image, as demonstrated in Figure 1c. While most area of the Pt substrate (~70%) was covered by clusters, only a certain fraction of the carbonaceous species nucleated to form graphene islands, either near a step edge or on a terrace.

The locations of the graphene islands were examined to identify the preferred nucleation sites of graphene. For example, Figure 2a shows a typical STM image of the graphene islands with the contrast enhanced in the derivative image (Figure 2b). The graphene islands are marked with either "S" or "T",

DOI: 10.1021/jp512163n
J. Phys. Chem. C 2015, 119, 7124–7129

corresponding to their locations (near a step edge or on a terrace). Thus, a statistical distribution of the graphene nucleation sites has been acquired over 300 graphene islands, as illustrated in Figure 2c, which indicates that about 60% of nucleation events occurred near a step edge and 40% on a terrace. This result implies that step edges are slightly preferred for graphene nucleation in this case. This agrees with previous studies suggesting that graphene nucleation is more favorable near a metal step edge than on a terrace,[8] as step edges can lower the energy barrier for graphene formation.[28] At high carbon concentrations, however, graphene nucleation occurs both near step edges and on terraces,[10] as observed here.

The nucleated graphene islands are mainly hexagonally shaped, with ~120° corners, regardless of their locations near a step edge or on a terrace, as shown in Figure 2. Therefore, the edges are all parallel to a specific crystallographic direction due to the 6-fold rotational symmetry of graphene lattice. Figure 3a shows another example of nucleated graphene islands, with an expanded view of an edge of a graphene island in Figure 3b, where the atomically resolved image indicates the atomically sharp zigzag structure as the preferred edge direction.[29−31] Similarly, the hexagonal graphene islands on the terraces mainly consist of zigzag edges, also supporting the notion that C-zigzag edges are the dominating edge type of graphene formed on Pt, Cu, and Co surfaces.[29,31] Theoretical calculations indeed confirm that zigzag edges have the lowest formation energy,[31] while the interaction with metal substrates may also play a key role in stabilizing the edge structures.

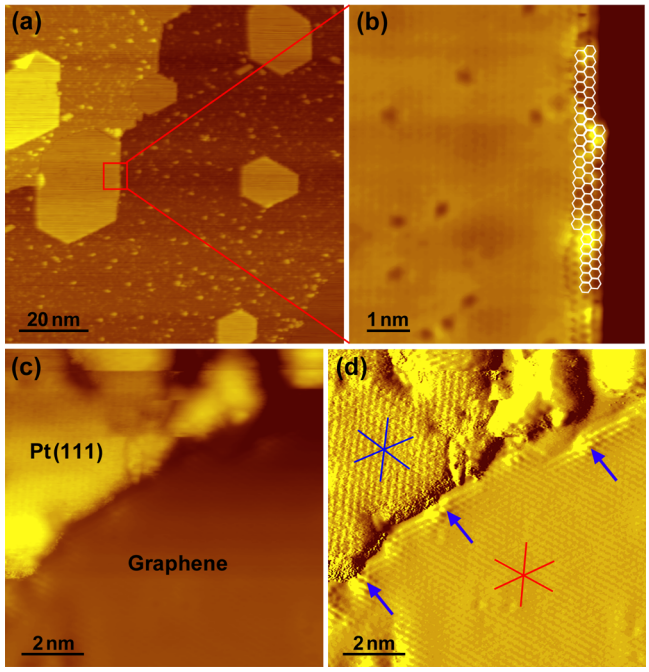

Figure 3. Edge structure and atomic lattice orientation of graphene islands grown on the flat Pt substrate using method 1. (a) An overview image of graphene islands on the Pt surface. (b) Expanded view of the zigzag edge structure enclosed by red square in (a). (c) STM topography of the graphene−Pt boundary. (d) Derivative image of (c), showing the atomic lattice structure of graphene and the Pt substrate. The lattice directions of graphene islands are found to be parallel to those of Pt substrate. The blue arrows indicate the strained graphene area near the border. Imaging parameters: (a) V_s = 300 mV, I_t = 14 pA; (b, c) V_s = 20 mV, I_t = 400 pA.

The interaction between graphene and Pt substrate plays a certain role in determining the structure and orientation of nucleated graphene islands. For example, the binding energy and charge transfer between graphene and metal substrate depend on the relative orientation between them.[32] Here we examined the relative lattice orientation between graphene islands and the Pt substrate to understand their interaction. Figure 3c shows the boundary area between a Pt terrace and a graphene island sitting on a lower terrace. The derivative STM image in Figure 3d enhances the resolution and helps resolve the atomic lattice structures for both the Pt substrate and the graphene island. It shows that the lattice orientations on the Pt substrate and on the graphene are parallel, as schematically illustrated by the crossing lines (blue for Pt substrate and red for graphene). More precisely, the rotational angle of graphene lattice relative to the Pt lattice is measured to be less than 1°. This alignment may give rise to a higher binding energy and is thus energetically favorable during graphene growth.[32] Nevertheless, rotated graphene domains are still possible due to thermal fluctuations, kinetic limitations, and inhomogeneities of metal substrate. This will result in graphene grains with different Moiré patterns[9,16] and the formation of grain boundaries that we discuss later.

In addition, the image in Figure 3d shows a contrast change near the graphene−Pt interface, as pointed out by arrows, which could indicate that the graphene lattice near the Pt boundary is strained and suggest a strong interaction between the growth frontier of the graphene island and adjacent Pt step.[33] Previous thermodynamic models suggest that the nucleation and growth of graphene islands on metal substrates involves an energetic cost due to the lattice mismatch between the metal step edges and graphene.[34] This strain energy could play an important role in graphene synthesis or coking processes.

The graphene−metal interaction is also manifested by the etching and faceting of metal steps during graphene growth. Figure 4a shows an STM image of graphene islands nucleated near Pt step edges. It reveals that graphene islands can grow by partially embedding into the upper Pt terrace, which implies that Pt atoms were etched away by the growing graphene. An expanded view of a graphene island is shown in Figure 4b with the atomic lattice structure revealed in the inset. A height profile along the red line and schematic illustration in Figure 4c present the step etching process by growing graphene. The graphene layer on Pt substrate shows an apparent height of around 1.2 Å, which is much smaller than the geometric spacing measured by low energy electron diffraction (3.7 Å).[22] This is due to an electronic effect;[35] that is, the density of states near Fermi level in graphene is much lower than that in Pt substrate, which forces the tip of the STM to be closer to the surface over the graphene areas. Metal etching during graphene growth on Ru and Au surfaces has been reported in previous studies.[13,36,37] Here, the observation of the faceting of Pt steps suggests that graphene prefers particular binding configurations at Pt steps. The hexagonal shapes of embedded graphene islands indicate that the graphene edges facing the Pt steps exhibit the zigzag termination, indicating that such configuration probably gives rise to a stronger binding between C and Pt steps.[38−40] This is manifested by a graphene film growth mode where Pt steps atoms are etched away, rather than growing over the top of Pt steps. This observation should have important implications in the coking of hydrocarbon reforming catalysts.

DOI: 10.1021/jp512163n
J. Phys. Chem. C 2015, 119, 7124−7129

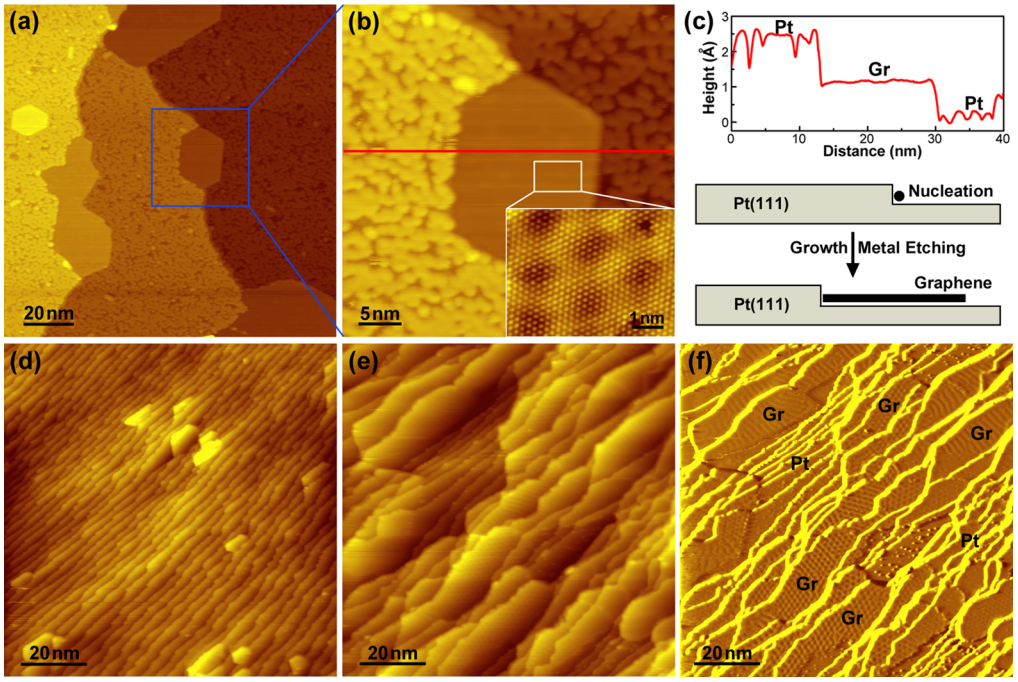

Figure 4. Graphene–Pt interaction during graphene growth on flat (a, b) and stepped (d–f) Pt substrates. The samples were prepared using method 1. (a, b) STM image showing a graphene island that partially etched into the Pt terrace. (c) Height profile along the red line in (b) and schematic illustration of metal etching during graphene growth. The measured height of graphene is strongly affected by the electronic density of states of graphene. (d) STM image of the stepped Pt(111) substrate with a terrace width of about 3 nm. (e) After graphene growth, some of the Pt terraces became broader. (f) Derivative image of (e), showing the Moiré patterns of graphene islands on the broad terraces. Imaging parameters: (a, b) V_s = 200 mV, I_t = 13 pA; inset in (b) V_s = 16 mV, I_t = 400 pA; (d, e) V_s = 500 mV, I_t = 14 pA.

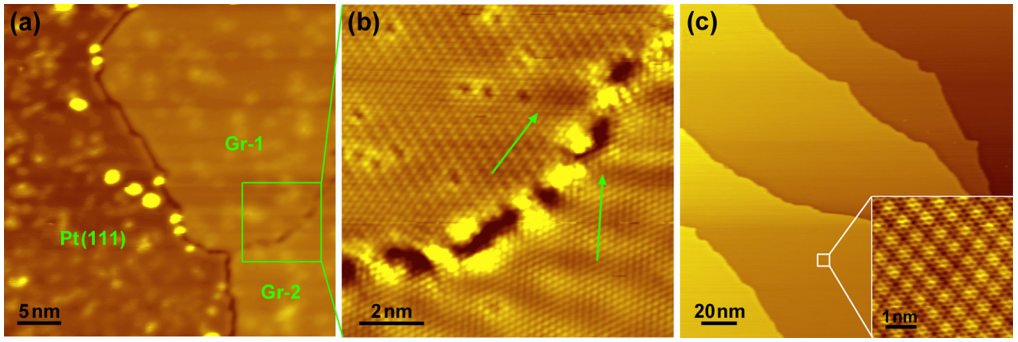

Figure 5. Grain boundary formation during graphene growth on the flat Pt substrate. (a) Two graphene islands merge with different lattice orientations, forming a grain boundary. The sample was grown using method 1. (b) An expanded view of the atomic structure near the boundary, where two grains are rotated ~27° with each other. (c) Growth method 2 produced a continuous high-quality graphene film over the Pt terraces, with atomic structure shown in the inset. Imaging parameters: (a, c) V_s = 200 mV, I_t = 14 pA; (b) V_s = 18 mV, I_t = 400 pA; inset in (c): V_s = 16 mV, I_t = 200 pA.

The etching and faceting of Pt steps during graphene growth were also examined on a highly stepped Pt surface. Figure 4d shows an STM image of a clean surface with an average terrace width ~3 nm. Such a dense step configuration is probably a better model for the surfaces of practical Pt catalysts in the form of small nanoparticles. After ethylene adsorption at room temperature followed by annealing to 1223 K, the surface reconstructed producing a certain broader terraces, as shown in Figure 4e. The image in Figure 4f, in derivative mode, confirms the formation of graphene islands, which can be distinguished by their Moiré patterns. The distribution of Pt terraces has changed: some are narrowed, while others are broadened and covered by graphene films. The reconstruction of Pt terraces was also caused by the etching of Pt steps during graphene growth. Compared to the relatively uniform orientation of graphene islands on the large terraces (Figure 1), the different Moiré patterns indicated a larger fraction of rotated graphene domains. This suggests that the orientation of graphene domains may depend on the graphene edge–metal interactions.[33] From the results of graphene growth on stepped Pt surface, it is reasonable to conclude that for practical materials such as Pt nanoparticles used in alkane dehydrogenation, coking processes likely will cause restructuring of the nanoparticles, with important implications for catalytic activity.

Epitaxial graphene films grown on metals are typically polycrystalline, consisting of single-crystalline grains connected by grain boundaries.[41–43] Grain boundaries may affect the properties of graphene film, such as weakening its mechanical strength and enhancing its chemical reactivity.[44–46] Understanding the formation of grain boundaries is helpful for

DOI: 10.1021/jp512163n
J. Phys. Chem. C 2015, 119, 7124–7129

controlled synthesis and applications of graphene. Generally grain boundaries are formed when two graphene grains merge with different lattice orientations.[41] Figure 5a shows one example of a grain boundary, where two graphene islands (marked with "Gr-1" and "Gr-2") joint to form a continuous layer. An expanded view in Figure 5b shows the atomic structure of the grain boundary, where the lattice orientations of the two grains are rotated with each other (~27° in this case). The connectivity between the two graphene grains varies along the boundary line, which might degrade the quality of the graphene sheet.[41]

Compared to the growth strategy followed above to prepare graphene films and study the nucleation, a second growth method was used consisting of directly exposing the Pt sample to ethylene at 1223 K for 2 min. Figure 5c shows a typical image of the produced graphene film using this method. The atomic lattice structure in the inset indicates a high quality of the graphene film. In this preparation method, graphene can grow across the steps forming a contiguous layer, in contrast with the metal-etching mode in which graphene is formed by thermally dissociating preadsorbed ethylene. The difference is that ethylene is adsorbed on a room temperature surface and dissociates and diffuses progressively as the temperature increases, a process that more likely corresponds to that of catalytic reactions.

The "hot" growth mode, leading to graphene carpeting over metal steps, has already been revealed by LEEM.[2] The key feature of the second method is that ethylene adsorbs on a hot surface well above the dissociation temperature, so that the diffusing entities are completely dehydrogenated carbon clusters. This leads to fewer nucleation centers (smaller nucleation density) and higher growth rate, allowing small graphene islands to grow large enough before they merge with other domains eventually. The nucleation and growth process can also be controlled by modifying the heating ramp rate.[47]

4. CONCLUSIONS

To summarize, we have presented a study on the growth mechanism of graphene on Pt surfaces using STM. We have shown that graphene growth by heating preadsorbed ethylene on Pt is very sensitive to graphene−Pt interaction. We have seen that nucleation occurs both near Pt step edges and on Pt terraces, producing hexagonal islands with atomically sharp zigzag edges. The atomic lattice orientations of the graphene islands are found to be parallel to those of the Pt substrate. The interaction of graphene with the Pt substrate during growth by annealing preadsorbed ethylene leads to the etching and faceting of Pt steps. However, when graphene is grown by directly exposing Pt to ethylene at high temperature, it forms a contiguous film, smoothly carpeting the metal surface over the atomic steps. These results contribute to a better understanding of the nucleation and growth of graphene on metal surfaces and have important implications on the structure and coking of Pt catalysts used in hydrocarbon reactions.

AUTHOR INFORMATION

Corresponding Author

*E-mail: mbsalmeron@lbl.gov (M.S.).

Present Address

X.F.: Department of Chemistry, Stanford University, Stanford, CA 94305.

Notes

The authors declare no competing financial interest.

ACKNOWLEDGMENTS

This work was supported by the Office of Basic Energy Sciences, Division of Materials Sciences and Engineering of the U.S. DOE, under Contract No. DE-AC02-05CH11231.

REFERENCES

(1) Geim, A. K.; Novoselov, K. S. The Rise of Graphene. *Nat. Mater.* **2007**, *6*, 183−191.
(2) Sutter, P. W.; Flege, J. I.; Sutter, E. A. Epitaxial Graphene on Ruthenium. *Nat. Mater.* **2008**, *7*, 406−411.
(3) Li, X.; Cai, W.; An, J.; Kim, S.; Nah, J.; Yang, D.; Piner, R.; Velamakanni, A.; Jung, I.; Tutuc, E.; et al. Large-Area Synthesis of High-Quality and Uniform Graphene Films on Copper Foils. *Science* **2009**, *324*, 1312−1314.
(4) Reina, A.; Jia, X.; Ho, J.; Nezich, D.; Son, H.; Bulovic, V.; Dresselhaus, M. S.; Kong, J. Large Area, Few-Layer Graphene Films on Arbitrary Substrates by Chemical Vapor Deposition. *Nano Lett.* **2009**, *9*, 30−35.
(5) Sutter, P.; Sadowski, J. T.; Sutter, E. Graphene on Pt(111): Growth and Substrate Interaction. *Phys. Rev. B* **2009**, *80*, 245411.
(6) Wintterlin, J.; Bocquet, M. L. Graphene on Metal Surfaces. *Surf. Sci.* **2009**, *603*, 1841−1852.
(7) Enachescu, M.; Schleef, D.; Ogletree, D. F.; Salmeron, M. Integration of Point-Contact Microscopy and Atomic-Force Microscopy: Application to Characterization of Graphite/Pt(111). *Phys. Rev. B* **1999**, *60*, 16913−16919.
(8) Gao, J.; Yip, J.; Zhao, J.; Yakobson, B. I.; Ding, F. Graphene Nucleation on Transition Metal Surface: Structure Transformation and Role of the Metal Step Edge. *J. Am. Chem. Soc.* **2011**, *133*, 5009−5015.
(9) Gao, M.; Pan, Y.; Huang, L.; Hu, H.; Zhang, L. Z.; Guo, H. M.; Du, S. X.; Gao, H. J. Epitaxial Growth and Structural Property of Graphene on Pt(111). *Appl. Phys. Lett.* **2011**, *98*, 033101.
(10) Loginova, E.; Bartelt, N. C.; Feibelman, P. J.; McCarty, K. F. Evidence for Graphene Growth by C Cluster Attachment. *New J. Phys.* **2008**, *10*, 093026.
(11) Loginova, E.; Bartelt, N. C.; Feibelman, P. J.; McCarty, K. F. Factors Influencing Graphene Growth on Metal Surfaces. *New J. Phys.* **2009**, *11*, 063046.
(12) Niu, T.; Zhou, M.; Zhang, J.; Feng, Y.; Chen, W. Growth Intermediates for CVD Graphene on Cu(111): Carbon Clusters and Defective Graphene. *J. Am. Chem. Soc.* **2013**, *135*, 8409−8414.
(13) Starodub, E.; Maier, S.; Stass, I.; Bartelt, N. C.; Feibelman, P. J.; Salmeron, M.; McCarty, K. F. Graphene Growth by Metal Etching on Ru(0001). *Phys. Rev. B* **2009**, *80*, 235422.
(14) Zhang, H.; Fu, Q.; Cui, Y.; Tan, D.; Bao, X. Growth Mechanism of Graphene on Ru(0001) and O_2 Adsorption on the Graphene/Ru(0001) Surface. *J. Phys. Chem. C* **2009**, *113*, 8296−8301.
(15) Cui, Y.; Fu, Q.; Bao, X. Dynamic Observation of Layer-by-Layer Growth and Removal of Graphene on Ru(0001). *Phys. Chem. Chem. Phys.* **2010**, *12*, 5053−5057.
(16) Merino, P.; Svec, M.; Pinardi, A. L.; Otero, G.; Martin-Gago, J. A. Strain-Driven Moiré Superstructures of Epitaxial Graphene on Transition Metal Surfaces. *ACS Nano* **2011**, *5*, 5627−5634.
(17) Seah, C. M.; Chai, S. P.; Mohamed, A. R. Mechanisms of Graphene Growth by Chemical Vapor Deposition on Transition Metals. *Carbon* **2014**, *70*, 1−21.
(18) Bartholomew, C. H. Mechanisms of Catalyst Deactivation. *Appl. Catal. A: Gen.* **2001**, *212*, 17−60.
(19) Wu, J.; Peng, Z.; Bell, A. T. Effects of Composition and Metal Particle Size on Ethane Dehydrogenation over Pt_xSn_{100-x}/Mg(Al)O ($70 \leq x \leq 100$). *J. Catal.* **2014**, *311*, 161−168.
(20) Peng, Z.; Somodi, F.; Helveg, S.; Kisielowski, C.; Specht, P.; Bell, A. T. High-Resolution In Situ and Ex Situ TEM Studies on

DOI: 10.1021/jp512163n
J. Phys. Chem. C 2015, 119, 7124−7129

Graphene Formation and Growth on Pt Nanoparticles. *J. Catal.* **2012**, *286*, 22−29.
(21) Wu, J.; Peng, Z.; Sun, P.; Bell, A. T. n-Butane Dehydrogenation over Pt/Mg(In)(Al)O. *Appl. Catal. A: Gen.* **2014**, *470*, 208−214.
(22) Zi-Pu, H.; Ogletree, D. F.; Van Hove, M. A.; Somorjai, G. A. LEED Theory for Incommensurate Overlayers: Application to Graphite on Pt(111). *Surf. Sci.* **1987**, *180*, 433−459.
(23) Land, T. A.; Michely, T.; Behm, R. J.; Hemminger, J. C.; Comsa, G. STM Investigation of Single Layer Graphite Structures Produced on Pt(111) by Hydrocarbon Decomposition. *Surf. Sci.* **1992**, *264*, 261−270.
(24) Land, T. A.; Michely, T.; Behm, R. J.; Hemminger, J. C.; Comsa, G. Direct Observation of Surface Reactions by Scanning Tunneling Microscopy: Ethylene → Ethylidyne → Carbon Particles → Graphite on Pt(111). *J. Chem. Phys.* **1992**, *97*, 6774−6783.
(25) Starr, D. E.; Pazhetnov, E. M.; Stadnichenko, A. I.; Boronin, A. I.; Shaikhutdinov, S. K. Carbon Films Grown on Pt(111) as Supports for Model Gold Catalysts. *Surf. Sci.* **2006**, *600*, 2688−2695.
(26) Johanek, V.; De La Ree, A. B.; Hemminger, J. C. Scanning Tunneling Microscopy Investigation of the Conversion of Ethylene to Carbon Clusters and Graphite on Pt(111). *J. Phys. Chem. C* **2009**, *113*, 4441−4444.
(27) Shimizu, T. K.; Mugarza, A.; Cerda, J. I.; Heyde, M.; Qi, Y. B.; Schwarz, U. D.; Ogletree, D. F.; Salmeron, M. Surface Species Formed by the Adsorption and Dissociation of Water Molecules on a Ru(0001) Surface Containing a Small Coverage of Carbon Atoms Studied by Scanning Tunneling Microscopy. *J. Phys. Chem. C* **2008**, *112*, 7445−7454.
(28) Bengaard, H. S.; Norskov, J. K.; Sehested, J.; Clausen, B. S.; Nielsen, L. P.; Molenbroek, A. M.; Rostrup-Nielsen, J. R. Steam Reforming and Graphite Formation on Ni Catalysts. *J. Catal.* **2002**, *209*, 365−384.
(29) Shu, H.; Chen, X.; Tao, X.; Ding, F. Edge Structural Stability and Kinetics of Graphene Chemical Vapor Deposition Growth. *ACS Nano* **2012**, *6*, 3243−3250.
(30) Zhang, X.; Yazyev, O. V.; Feng, J.; Xie, L.; Tao, C.; Chen, Y. C.; Jiao, L.; Pedramrazi, Z.; Zettl, A.; Louie, S. G.; et al. Experimentally Engineering the Edge Termination of Graphene Nanoribbons. *ACS Nano* **2013**, *7*, 198−202.
(31) Prezzi, D.; Eom, D.; Rim, K. T.; Zhou, H.; Xiao, S.; Nuckolls, C.; Heinz, T. F.; Flynn, G. W.; Hybertsen, M. S. Edge Structures for Nanoscale Graphene Islands on Co(0001) Surfaces. *ACS Nano* **2014**, *8*, 5765−5773.
(32) Kappes, B. B.; Ebnonnasir, A.; Kodambaka, S.; Ciobanu, C. V. Orientation-Dependent Binding Energy of Graphene on Palladium. *Appl. Phys. Lett.* **2013**, *102*, 051606.
(33) Zhang, X.; Xu, Z.; Hui, L.; Xin, J.; Ding, F. How the Orientation of Graphene is Determined during Chemical Vapor Deposition Growth. *J. Phys. Chem. Lett.* **2012**, *3*, 2822−2827.
(34) Saadi, S.; Abild-Pedersen, F.; Helveg, S.; Sehested, J.; Hinnemann, B.; Appel, C. C.; Norskov, J. K. On the Role of Metal Step-Edges in Graphene Growth. *J. Phys. Chem. C* **2010**, *114*, 11221−11227.
(35) Feng, X.; Salmeron, M. Electronic Screening in Stacked Graphene Flakes Revealed by Scanning Tunneling Microscopy. *Appl. Phys. Lett.* **2013**, *102*, 053116.
(36) Gunther, S.; Danhardt, S.; Wang, B.; Bocquet, M. L.; Schmitt, S.; Wintterlin, J. Single Terrace Growth of Graphene on a Metal Surface. *Nano Lett.* **2011**, *11*, 1895−1900.
(37) Nie, S.; Bartelt, N. C.; Wofford, J. M.; Dubon, O. D.; McCarty, K. F.; Thurmer, K. Scanning Tunneling Microscopy Study of Graphene on Au(111): Growth Mechanisms and Substrate Interactions. *Phys. Rev. B* **2012**, *85*, 205406.
(38) Patera, L. L.; Africh, C.; Weatherup, R. S.; Blume, R.; Bhardwaj, S.; Castellarin-Cudia, C.; Knop-Gericke, A.; Schloegl, R.; Comelli, G.; Hofmann, S.; et al. In Situ Observations of the Atomistic Mechanisms of Ni Catalyzed Low Temperature Graphene Growth. *ACS Nano* **2013**, *7*, 7901−7912.
(39) Kim, H. W.; Ku, J.; Ko, W.; Jeon, I.; Kwon, H.; Ryu, S.; Kahng, S. J.; Lee, S. H.; Hwang, S. W.; Suh, H. Strong Interaction between Graphene Edge and Metal Revealed by Scanning Tunneling Microscopy. *Carbon* **2014**, *78*, 190−195.
(40) Chen, H.; Zhu, W.; Zhang, Z. Contrasting Behavior of Carbon Nucleation in the Initial Stages of Graphene Epitaxial Growth on Stepped Metal Surfaces. *Phys. Rev. Lett.* **2010**, *104*, 186101.
(41) Huang, P. Y.; Ruiz-Vargas, C. S.; van der Zande, A. M.; Whitney, W. S.; Levendorf, M. P.; Kevek, J. W.; Garg, S.; Alden, J. S.; Hustedt, C. J.; Zhu, Y.; et al. Grains and Grain Boundaries in Single-Layer Graphene Atomic Patchwork Quilts. *Nature* **2011**, *469*, 389−392.
(42) Nemes-Incze, P.; Yoo, K. J.; Tapaszto, L.; Dobrik, G.; Labar, J.; Horvath, Z. E.; Hwang, C.; Biro, L. P. Revealing the Grain Structure of Graphene Grown by Chemical Vapor Deposition. *Appl. Phys. Lett.* **2011**, *99*, 023104.
(43) Ogawa, Y.; Hu, B.; Orofeo, C. M.; Tsuji, M.; Ikeda, K.; Mizuno, S.; Hibino, H.; Ago, H. Domain Structure and Boundary in Single-Layer Graphene Grown on Cu(111) and Cu(100) Films. *J. Phys. Chem. Lett.* **2012**, *3*, 219−226.
(44) Feng, X.; Maier, S.; Salmeron, M. Water Splits Epitaxial Graphene and Intercalates. *J. Am. Chem. Soc.* **2012**, *134*, 5662−5668.
(45) Liang, Z.; Khosravian, H.; Uhl, A.; Meyer, R. J.; Trenary, M. Graphene Domain Boundaries on Pt(111) as Nucleation Sites for Pt Nanocluster Formation. *Surf. Sci.* **2012**, *606*, 1643−1648.
(46) Biro, L. P.; Lambin, P. Grain Boundaries in Graphene Grown by Chemical Vapor Deposition. *New J. Phys.* **2013**, *15*, 035024.
(47) Jung, D. H.; Kang, C.; Son, B. H.; Ahn, Y. H.; Lee, J. S. Correlating Nucleation Density with Heating Ramp Rates in Continuous Graphene Film Formation. *Carbon* **2014**, *80*, 708−715.

DOI: 10.1021/jp512163n
J. Phys. Chem. C 2015, 119, 7124−7129